

A Low Profile Miniaturization Low Frequency Wideband Antenna Using Passive Lumped Elements Loading

Yinfeng Xia¹, Yingsong Li^{1,2*}, and Wei Xue¹

¹ College of Information and Communication Engineering
Harbin Engineering University, Harbin150001, China
*liyingsong@ieee.org

² Key Laboratory of Microwave Remote Sensing
National Space Science Center
Chinese Academy of Sciences, Beijing 100190, China

Abstract — In this paper, a low profile miniaturization low frequency sleeve monopole antenna loaded with passive lumped (PL) elements is proposed, which can be utilized for HF, VHF, UHF, and P band applications. The proposed antenna is fed by coplanar waveguide (CPW) and composed of feeding line, modified T-shaped radiation patch, sleeve structure and loaded passive lumped elements. An original monopole antenna is operating at 231 MHz with a small fractional bandwidth of 31.8%. By modifying the T-shaped radiation patch and adding the sleeve structure, the fractional bandwidth can be improved by 11%. To further enhance its performance, several passive lumped elements are integrated with the antenna. The design procedure is presented and analyzed in detail. The simulated results demonstrate that a fractional bandwidth of 192.2% from 10-500 MHz can be achieved for the proposed antenna system, which is also in agreement with the measured result.

Index Terms — Low profile, miniaturization, passive loading, ultra-wideband.

I. INTRODUCTION

High data transmission, miniaturization, multifunction wireless communication system has become a hot topic in the modern wireless communication system development. To meet the demands, antenna, as an intrinsic and essential component of wireless communication system, is also developing toward the same tendency. Multiband antennas can support many sub-systems and then realize multifunction [1-3]. However, more communication frequency bands are required with the increasing of functions of devices, which will make the antenna design more difficult. MIMO antenna array may also be a good choice to improve data transmission. Yet, strong coupling will be inevitable between the MIMO antenna array elements

and extra decoupling work is needed to reduce the mutual interferences [4-5]. To solve these problems and meet the wireless communication system developing tendency, miniaturization wideband antenna may be one of the best options.

Nonetheless, the miniaturization of antenna is contradictory with the bandwidth especially at low frequency [6-7]. As is known to us, low frequency antennas usually exist with the form of large size, which is related to its wavelength. Decreasing the size of low frequency antennas will degrade its performance. To trade-off the contradiction, many methods have been proposed [8-13]. So far, the most popular method is to utilize the non-foster circuit (NFC) to match an electrically small antenna (ESA) [13]. In [14-19], NFC matched ESAs have been reported. However, in most of the reported literatures, the bandwidth has been improved, which just compared with the bandwidth of antenna itself resonance. Thus, the achieved bandwidth of these antennas is not enough to cover wide low frequency band, such as for HF, VHF, UHF applications together. In [19], a fractional of 169% from 18 MHz to 218 MHz has been obtained, which is also using the NFC matching method. Yet, the proposed antenna has a height of 30 cm and a ground plane of 20×16 cm², which will occupy large volume for the wireless communication system. Therefore, designing a low profile, miniaturization, wideband antenna for low frequency wireless communication is urgent and indispensable.

In this paper, a miniaturization low profile planar sleeve monopole antenna is proposed, which is realized with passive lumped element loading. The proposed antenna is fed by CPW and composed of modified T-shaped radiation patch, feeding line, ground plane and loaded with passive lumped elements. The original model of the proposed antenna operates at 231 MHz with a small fractional bandwidth of 31.8%. To improve its bandwidth, the T-shaped radiation patch is modified, and

sleeve structure is introduced into the antenna structure to improve its performance a little. To further enhance its bandwidth, lumped elements are integrated to the antenna structure. By properly optimizing the structure and adjusting the values of these lumped elements, a -10 dB fractional bandwidth of 192.2% from 10-500 MHz can be obtained. Moreover, the measured result is in agreement with the simulated one.

II. DESIGN OF THE PROPOSED ANTENNA

In this section, the design procedure of the proposed antenna is presented, which can be developed by three steps. Each step is corresponded with an antenna model. By analyzing the antenna models, the design principle can be well understood.

A. Design of the antenna 1

The structure of the antenna 1 is depicted in Fig. 1, where the top view and side view are given, respectively. The designed antenna 1 is fed by coplanar waveguide composed (CPW) and composed of feeding line, T-shaped radiation patch, part ground plane, which is printed on a FR4 substrate with a relative permittivity of 4.4, a loss tangent of 0.02 and a thickness of $h=1.6$ mm. The antenna 1, as the original antenna, is a monopole-like antenna. The entire size of the antenna is $W1 \times L1 = 330 \times 320$ mm². The width S of the feeding line and the gap g between the feeding line and the part ground plane are calculated and obtained from CPW structure theory [20], which are set 3 mm and 0.5 mm, respectively. To enhance the -10 dB bandwidth of the antenna 1, it is optimized in the HFSS. The optimized dimensions are: $W2=100$ mm, $W3=120$ mm, $L2=300$ mm, and $L3=50$ mm.

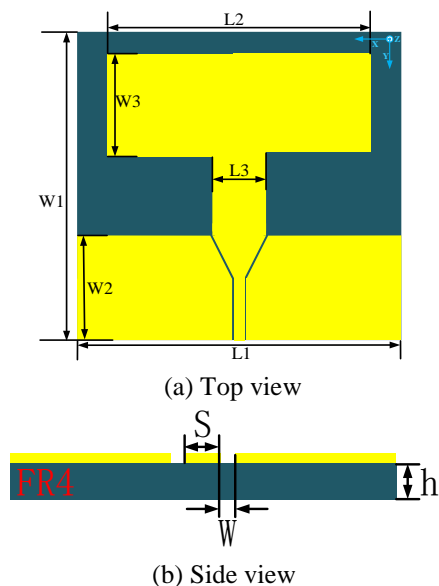


Fig. 1. The geometry of the designed antenna 1.

The performance of the designed antenna 1 is given in Figs. 2 and 3, where the simulated reflection coefficient (S_{11}) and the simulated radiation patterns are presented, respectively. From Fig. 2, it can be concluded that the designed antenna 1 operates at 231 MHz with a -10 dB fractional bandwidth of 31.8%. Moreover, the antenna 1 has an omnidirectional radiation pattern, which is depicted in Fig. 3.

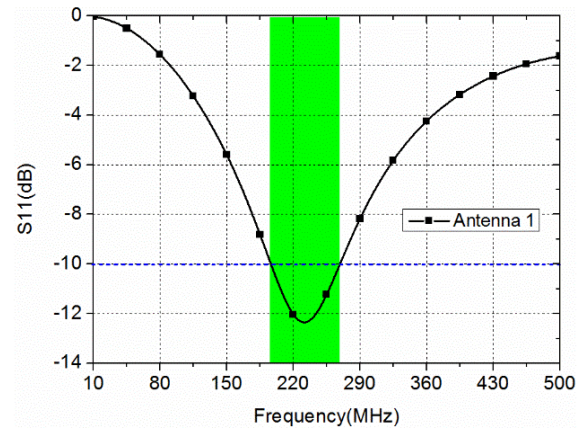


Fig. 2. The simulated S_{11} of the designed antenna 1.

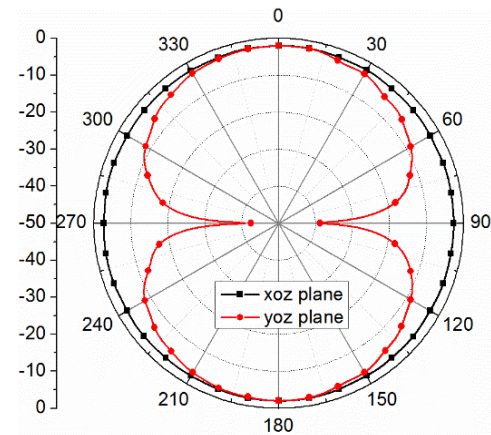


Fig. 3. The radiation patterns of designed antenna 1.

To understand the principle of the antenna 1, the current distribution is shown in Fig. 4. From Fig. 4, it can be observed that the current is mainly distributed on the feeding line, the ground plane, the T-shaped radiation patch. Based on the simulated current distribution, the size of the T-shaped radiation patch can be optimized to enhance its performance. To analyze the effects on the resonance of the antenna, key parameters of the patch are selected to analyze and investigate the effects on the performance of the designed antenna 1. The simulated results are given in Figs. 5 and 6.

The width $L2$ and the length $W3$ of the T-shaped radiation patch are selected to analyze its effects on the

performance of the designed antenna 1. The T-shaped radiation patch is composed of a rectangle patch marked by L2, W3 and a line marked by L3. In fact, increasing the values of W3 or L2 can improve the bandwidth of the antenna 1 which is given in Figs. 5 and 6. From Fig. 5, it can be observed that the center resonance frequency shifts toward to lower frequency and the -10 dB bandwidth can also be improved a little with the increasing of L2. Also, the same conclusion can be draw from the Fig. 6, which is that the center resonance frequency shifts toward to higher frequency band and the -10 dB bandwidth can also be improved a little with the increasing of W3. Thus, properly optimizing both parameters can control the center resonance frequency and bandwidth of the designed antenna 1.

Based on the analysis for the designed antenna 1, it can be concluded that the bandwidth of the antenna 1 can be improved by optimizing the dimensions of the designed antenna 1. To make the structure more compact, the width L2 is set by 300 mm, and the length W3 is optimized to improve the performance of the antenna 1. To enhance the bandwidth of the antenna 1, the antenna 2 is developed, which is based on the configuration of antenna 1 and integrates the sleeve theory.

B. Design of the antenna 2

The configuration of the developed antenna 2 is presented in Fig. 7, which has the same basic structure with the designed antenna 1. In addition, the T-shaped radiation patch is modified by adding two pairs of parasitic branches. Two sleeve structures are also connected to the ground plane, which is beneficial to improve the impedance matching for the designed antenna 1.

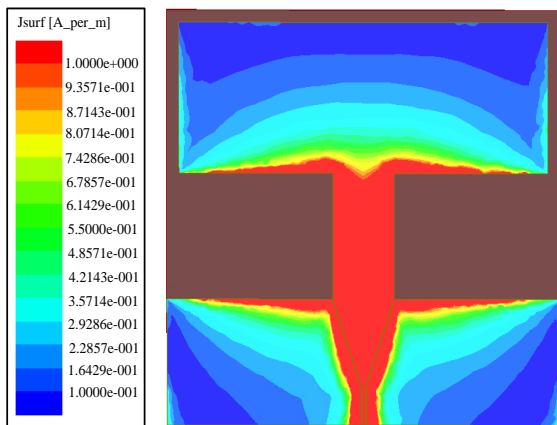


Fig. 4. The current distribution of designed antenna 1.

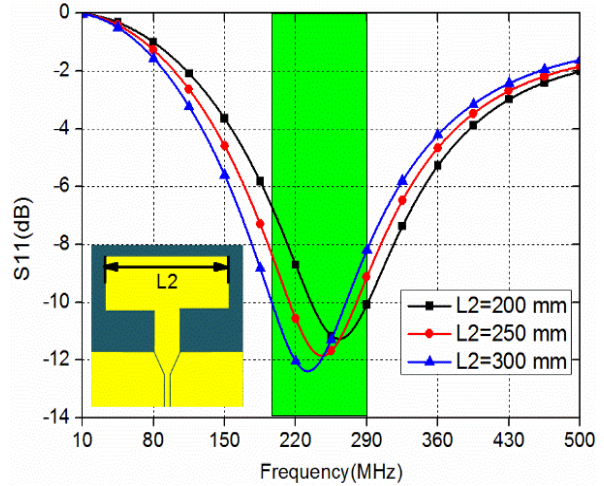


Fig. 5. The effect of L2 on the performance of the designed antenna 1.

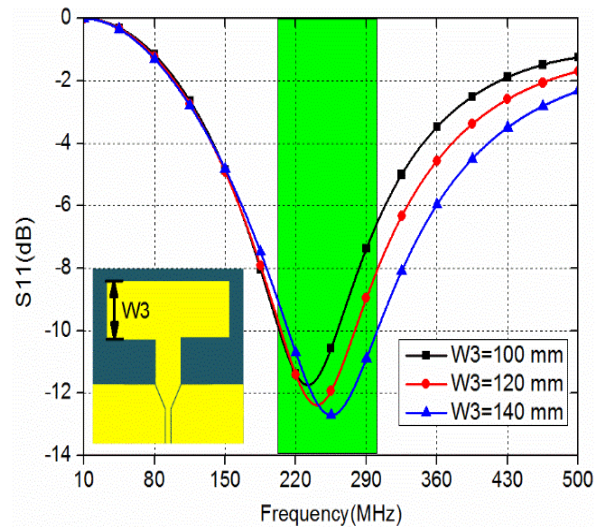


Fig. 6. The effect of W3 on the performance of the designed antenna 1.

The simulated reflection coefficient (S11) is depicted in Fig. 8, which indicates that the antenna 2 has a -10 dB fractional bandwidth of 42.8% covering from 180 MHz to 278 MHz. By comparing with the result of the designed antenna 1, it can be concluded that the fractional bandwidth has been improved by 11%. Moreover, the developed antenna 2 has also an omnidirectional radiation patterns presented in Fig. 9. However, the peak gain has been decreased by 0.39 dBi for the developed antenna 2.

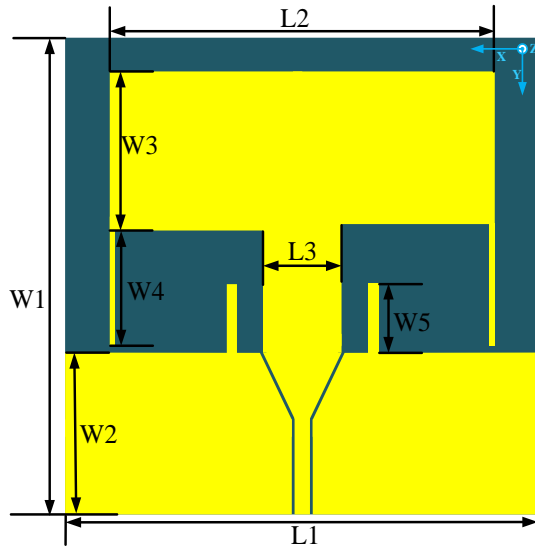


Fig. 7. The configuration of the designed antenna 2.

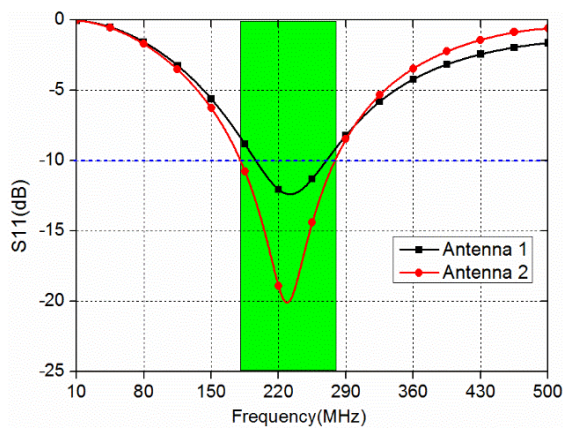


Fig. 8. S11 comparison of antenna 1 and antenna 2.

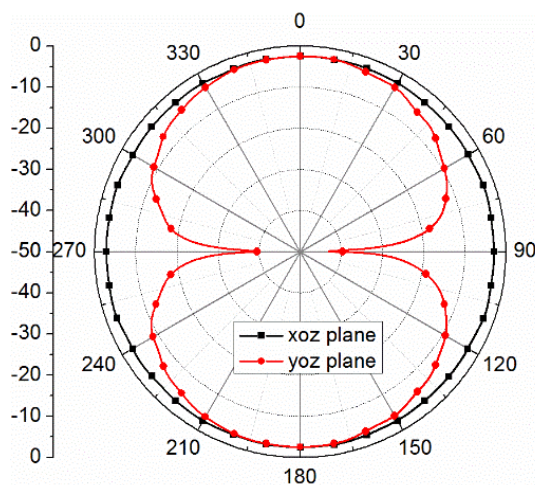


Fig. 9. The radiation patterns of devised antenna 2.

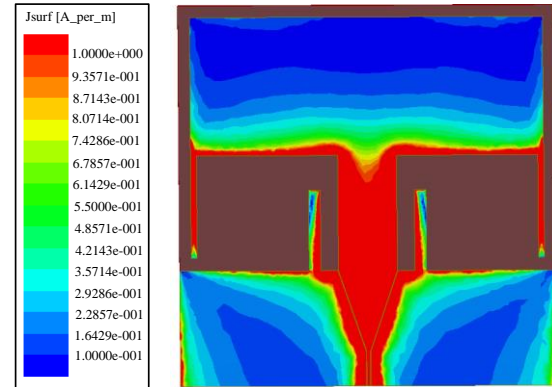


Fig. 10. The current distribution of the devised antenna 2.

The current distribution of the devised antenna 2 is given in Fig. 10, which can give an understanding for the antenna 2 design. From the current distribution, it can be seen that the current distribution concentrates on the feeding line, the ground plane, the T-shaped radiation patch, the parasitic branches and the sleeve structure. The parasitic branches and sleeve structure integrated into the designed antenna 1 can prolong the current path, which can be equivalent to the inductor loading to cancel the resistance of designed antenna 1. Thereby, the bandwidth of antenna 1 can be enhanced.

Although the bandwidth of the developed antenna 2 has achieved a -10 dB fractional bandwidth of 42.8%, it still cannot meet the demand of modern broadband wireless communication for wide range of detection at low frequency. To solve the problems and further enhance the bandwidth of the antenna 2, the antenna 3 is proposed as the final design of the low frequency wide band antenna.

C. Design of the antenna 3

The geometry of the antenna 3 is shown in Fig. 11, where passive lumped elements are integrated into the antenna structure that is based on the configuration of the designed antenna 2. These passive lumped elements include an inductor, a capacitance, and five resistances. The parasitic branches are connected to the ground by both resistance R4 and R5. The sleeve structures are attached with the T-shaped patch by both resistance R2 and R3. The resistance R1 and the inductor L1 are incorporated into the feeding line. While the capacitance C1 is set at the bottom of the substrate, which will make the soldering more convenient. The inductor L1 and the capacitance C1 are selected to make the proposed 3 resonate at high frequency band. And, five resistances R1, R2, R3, R4, and R5 are chosen to make the proposed antenna match to 50Ω . Thus, the bandwidth of the original antenna can be greatly enhanced by properly adjusting these elements in the HFSS.

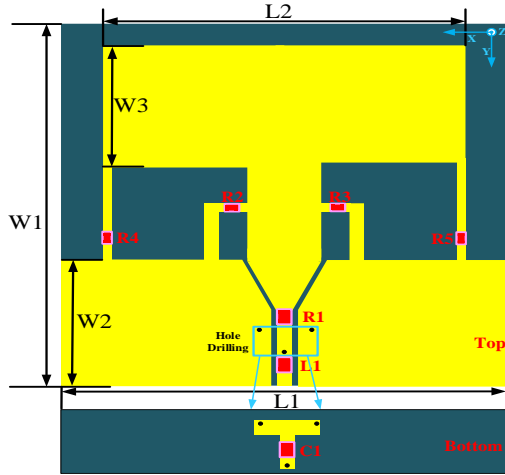


Fig. 11. The geometry of devised antenna 3.

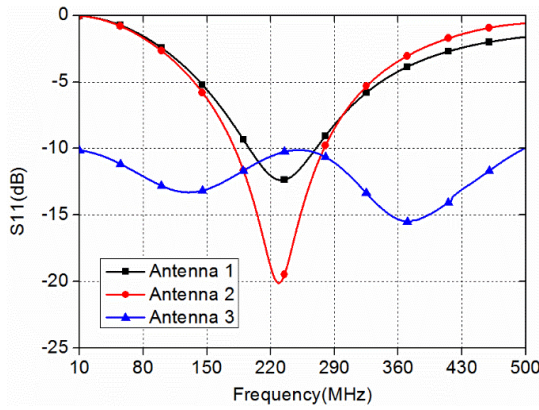


Fig. 12. Comparison of S11 for the designed three antennas.

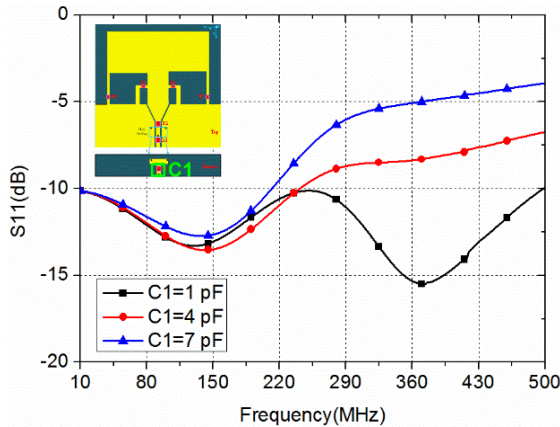


Fig. 13. The effect of C1 on the performance of the devised antenna 3.

The devised antenna 3 is modeled and optimized by the HFSS. By properly adjusting these values of the

lumped elements, an ultra-wideband wideband can be obtained and named as antenna 3. And, the simulated reflection coefficients (S11s) is presented in Fig. 12, where the devised antenna 3 can achieve a -10 dB fractional bandwidth of 192.2% ranging from 10 MHz to 500 MHz that has been enhanced greatly in comparison with the simulated S11 of antenna 1 and antenna 2.

III. ANALYSIS AND MEASUREMENT

The final designed antenna 3 and its performance are depicted herein. To analyze the design principle, two parameters (the capacitance C1 and the resistance R1) are selected to investigate the effects for the finalized antenna 3. The results are show in Figs. 13 and 14. From Fig. 13, it can be observed that the bandwidth of the designed antenna has been deceased with the increasing of C1, especially, which means that C1 has great effect on the higher frequency band. Similarly, the inductor L1 has the same effect on the antenna 3. From Fig. 14, it can be concluded that the R1 has great effect for the antenna 3 in the entire frequency band. The three elements, namely C1, L1, and R1, are the most sensitive components. Thus, properly optimizing the three key elements and then adjusting the other four resistances can obtain a good performance for the antenna 3.

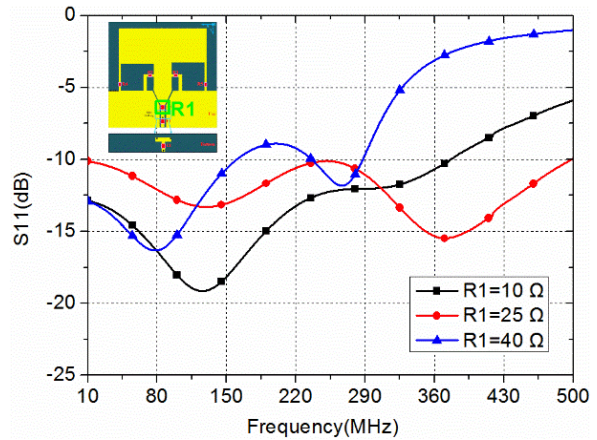


Fig. 14. The effect of R1 on the performance of the devised antenna 3.



Fig. 15. The photograph of the fabricated antenna.

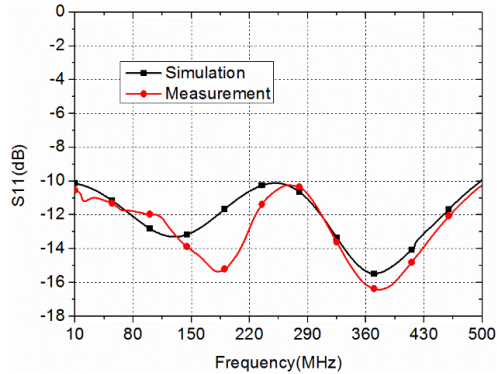


Fig. 16. Comparison of S11 of the simulation and measurement.

At last, to validate the simulated results, the antenna 3 is fabricated and these passive lumped elements are soldered into the fabricated antenna, which is shown in Fig. 15. To improve the accuracy of the experiment, these passive elements are used with the high accuracy of 1%. The reflection coefficient (S11) of the fabricated antenna is measured by employing the Keysight ENA Series Network Analyzer E5061B. The comparison of the simulated and measured results is depicted in Fig. 16.

From the Fig. 16, it can be concluded that the fabricated antenna has also a -10 dB fractional bandwidth of 192.2% ranging from 10 MHz to 500 MHz, which is in agreement with the simulated result. However, there is some difference between the simulation and measurement, which may be caused by the fabrication error, the parasitic effects of the electronic components, the soldering and stability of the substrate. To better evaluate the performance of the proposed antenna, the measured total efficiency and radiation patterns may be needed. However, the operating frequency band at low frequency is difficult to measure in practical, which means that an extremely large anechoic chamber is required for the measurement. In fact, it is difficult to measure the radiation patterns at very low frequency.

IV. CONCLUSION

In this paper, a low profile miniaturization sleeve monopole antenna loaded with passive lumped elements is proposed, which can be utilized for HF, VHF, UHF, and P band applications. The proposed antenna is divided into three antenna models to discuss the design procedure. The performance of each antenna model is analyzed in detail. The bandwidth of the proposed antenna has been improved step by step. At last, the final designed antenna loaded with lumped elements achieves a -10 dB fractional bandwidth of 192.2% ranging from 10 MHz to 500 MHz, which is greatly enhanced comparing with the results of the former two designed antennas. Moreover, the measured result is in agreement with the simulated one.

In the future, the metasurface and filtering methods [21-23] can be well investigated on such antenna development, and the wide bandwidth beamforming based on adaptive techniques [24-28] is still an amazing topic.

ACKNOWLEDGMENTS

This paper is supported by the National Key Research and Development Program of China (2016YFE0111100), Key Research and Development Program of Heilongjiang (GX17A016), the Science and Technology innovative Talents Foundation of Harbin (2016RAXXJ044), the Natural Science Foundation of Beijing (4182077), China Postdoctoral Science Foundation (2017M620918, 2019T120134), the Fundamental Research Funds for the Central Universities (HEUCFG201829, 2072019CFG0801), and Opening Fund of Acoustics Science and Technology Laboratory (SSKF2016001).

REFERENCES

- [1] D. G. Lopez, M. Ignatenko, and D. S. Filipovic, "Low-profile tri-band inverted-F antenna for vehicular applications in HF and VHF bands," *IEEE Trans. Antennas Propag.*, vol. 63, no. 11, pp. 4632-4639, Nov. 2015.
- [2] Y. Xia, W. Xue, Y. Li, and L. Zhao, "A dual-band WLAN antenna with reactive loading," *Applied Computational Electromagnetics Society Journal*, vol. 34, no. 7, pp. 1026-1031, July 2019.
- [3] W. An, X. Wang, H. Fu, J. Ma, X. Huang, and B. Feng, "Low-profile wideband slot-loaded patch antenna with multiresonant modes," *IEEE Antennas Wireless Propag Lett.*, vol. 17, no. 7, pp. 1309-1313, Jul. 2018.
- [4] J. Jiang, Y. Xia, and Y. Li, "High isolated X-band MIMO array using novel wheel-like metamaterial decoupling structure," *Applied Computational Electromagnetics Society Journal*, accepted 2020.
- [5] S. Luo, Y. Li, Y. Xia, and L. Zhang, "A low mutual coupling antenna array with gain enhancement using metamaterial loading and neutralization line structure," *Applied Computational Electromagnetics Society Journal*, vol. 34, no. 3, pp. 411-418, Mar. 2019.
- [6] L. J. Chu, "Physical limitations of omni-directional antennas," *J. Appl. Phys.*, vol. 19, no. 12, pp. 1163-1175, May 1948.
- [7] A. D. Yaghjian and S. R. Best, "Impedance, bandwidth, and Q of antennas," *IEEE Trans. Antennas Propag.*, vol. 53, no. 4, pp. 1298-1324, Aug. 2005.
- [8] R. W. Ziolkowski, "An efficient, electrically small antenna designed for VHF and UHF applications," *IEEE Antennas Wireless Propag Lett.*, vol. 7, pp. 217-220, Apr. 2008.
- [9] L. Mattioni and G. Marrocco, "Design of a

- broadband HF antenna for multimode naval communications-part II: extension to VHF/UHF ranges,” *IEEE Antennas Wireless Propag Lett.*, vol. 6, pp. 83-85, Mar. 2007.
- [10] K. Ghaemi and N. Behdad, “A low-profile, vertically polarized ultrawideband antenna with monopole-like radiation characteristics,” *IEEE Trans. Antennas Propag.*, vol. 63, no. 8, pp. 3699-3705, Aug. 2015.
- [11] A. Loutridis, “Study of UHF and VHF compact antennas,” *Ph.D. Thesis*, Dublin Institute of Technology, Ireland, 2015.
- [12] K. Ghaemi, R. Ma, and N. Behdad, “A small-aperture, ultrawideband HF/VHF direction-finding system for unmanned aerial vehicles,” *IEEE Trans. Antennas Propag.*, vol. 66, no. 10, pp. 5109-5120, Oct. 2018.
- [13] J. T. Aberle, “Two-port representation of an antenna with application to non-foster matching networks,” *IEEE Trans. Antennas Propag.*, vol. 56, no. 5, pp. 1218-1222, May 2008.
- [14] J. Church, J. C. S. Chieh, L. Xu, J. D. Rockway, and D. Arceo, “UHF electrically small box cage loop antenna with an embedded non-Foster load,” *IEEE Antennas Wireless Propag. Lett.*, vol. 13, pp. 1329-1332, Jul. 2014.
- [15] Y. Xia, Y. Li, and S. Zhang, “A non-foster matching circuit for an ultra-wideband electrically small antenna,” *13th European Conference on Antennas and Propagation*, Krakow, Poland, 2019.
- [16] T. Shi, M. Tang, Z. Wu, H. Xu, and R. W. Ziolkowski, “Improved signal-to-noise ratio, bandwidth-enhanced electrically small antenna augmented with internal non-Foster elements,” *IEEE Trans. Antennas Propag.*, vol. 67, no. 4, pp. 2763-2768, Jan. 2019.
- [17] C. R. White, J. S. Colburn, and R. G. Nagele, “A non-foster VHF monopole antenna,” *IEEE Antennas Wireless Propag Lett.*, vol. 11, pp. 584-587, Jun. 2012.
- [18] M. M. Jacob and D. F. Sievenpiper, “Non-foster matched antennas for high-power applications,” *IEEE Trans. Antennas Propag.*, vol. 65, no. 9, pp. 4461-4469, Sept. 2017.
- [19] Y. Xia, W. Xue, Y. Li, W. Shi, and B. Li “A low frequency ultra-wideband electrically small monopole antenna for HF/VHF application,” *Applied Computational Electromagnetics Society Journal*, vol. 34, no. 7, pp. 1050-1057, Jul. 2019.
- [20] R. N. Simons, *Coplanar Waveguide Circuits, Components and Systems*, New York: John Wiley & Sons, 2004.
- [21] K. Yu, Y. Li, and X. Liu, “Mutual coupling reduction of a MIMO antenna array using 3-D novel meta-material structures,” *Applied Computational Electromagnetics Society Journal*, vol. 33, no. 7, pp. 758-763, Jul. 2018.
- [22] F. Liu, J. Guo, L. Zhao, et al., “Dual-band meta-surface-based decoupling method for two closely packed dual-band antennas,” *IEEE Transactions on Antennas and Propagation*, 10.1109/TAP.2019.2940316, 2019.
- [23] W. Wang, J. Ran, N. Hu, W. Xie, Y. Wu, and A. Kishk, “A novel differential filtering patch antenna with high selectivity,” *International Journal of RF and Microwave Computer-Aided Engineering*, vol. 29, no. 10, e21880, Oct. 2019.
- [24] X. Zhang, T. Jiang, Y. Li, et al., “A novel block sparse reconstruction method for DOA estimation with unknown mutual coupling,” *IEEE Communications Letters*, vol. 23, no. 10, pp. 1845-1848, 2019.
- [25] Y. Li, Z. Jiang, O. M. O. Osman, et al., “Mixed norm constrained sparse APA algorithm for satellite and network echo channel estimation,” *IEEE Access*, vol. 6, pp. 65901-65908, 2018.
- [26] Y. Li, Z. Jiang, W. Shi, et al., “Blocked maximum correntropy criterion algorithm for cluster-sparse system identifications,” *IEEE Transactions on Circuits and Systems II: Express Briefs*, vol. 66, no. 11, pp. 1915-1919, 2019.
- [27] W. Shi, Y. Li, and L. Zhao, “Controllable sparse antenna array for adaptive beamforming,” *IEEE Access*, vol. 7, pp. 6412-6423, 2019.
- [28] W. Shi, Y. Li, and Y. Wang, “Noise-free maximum correntropy criterion algorithm in non-gaussian environment,” *IEEE Transactions on Circuits and Systems II: Express Briefs*, 10.1109/TCSII.2019.2914511, 2019.